論文 한국정밀공학회지 제12권 제7호 1995. 7
Journal of the Korean Society of Precision Engineering Vol. 12. No7. July. 1995.

회전유동의 입자화상처리시 광학적 해석

김 유 곤*

Optical Analysis in Particle Image Processing of Rotating Flow

You-Gon Kim*

ABSTRACT

입자화상 처리기법은 유체역학 분야의 정량적 유동가시화에 있어서 중요한 역할을 하고 있다. 회전유동의 측면 사진을 찍을 때, 측정부의 볼록면 때문에 그 영상에서 광학적 변형이 일어나게 된다. 이러한 변형은 측정부의 형상은 물론 회전유동의 방향에 의해서도 큰 영향을 받는다. 정확한 유동장을 얻기 위해서 이러한 변형이 적절한 방법에 의하여 교정된다. 교정한 실험 데이터를 수치해석 결과와 비교해 보면 정량적으로 잘 맞는 것을 알 수 있다.

Key Words : Particle Image Processing(입자화상처리), Quantitative Flow Visualization(정량적 유동 가시화), Rotating Flow(회전유동), Optical Distortion(광학적 변형), Digital Vector Velocimetry (DVV;디지탈 벡터 속도계)

1. Introduction

Recent advances in optics, electronics and imaging technique make a quantitative flow visualization[1,2] of velocity field possible. These advances allow one to capture the instantaneous Eulerian velocity images for a flow field. In addition, one may take advantage of a digital data processing system to derive additional information such as streamlines, vorticity distribution, pressure field, skin friction, and drag forces. Quantitative flow visualization attracts many investigations because of its ability to measure velocity vectors at multipoints of a flow field at the same time. Furthermore, it needs much less effort and time comparing with single-point measurement such as hot wire and laser Doppler anemometries.

In the present study, which has been conducted in the University of Iowa, a quantitative flow imaging technique, called the digital vector velocimetry (DVV) method,[3,4,5] is employed to measure the velocity field in the

* 전남대학교 기계공학과

lid-driven rotating flow. Rotating flows are in general three dimensional and the flow fields are very difficult to measure due to curved geometry normally associated with the rotating flow. Therefore, there is a definite need to develop a measuring device and technique to obtain the comprehensive data of velocity field and for the rotating flow. The present study may produce benchmark data for basic lid-driven internal, rotating flows of the rotor-stator systems. The measurements made by the DVV method for the steady rotating flow are then compared with results of numerical simulation employing the Finite Analytic method (FAM).[6,7]

The digital vector velocimetry (DVV) method is a method to achieve multipoint quantitative measurement of a flow field. The DVV method invokes the idea of the most probable particle translation between two time-sequential images by constructing a velocity vectorgram from them for a selected small interrogating element. A procedure is conceived to identify the most probable intense digital vector to be the velocity vector for the fluid in the element. Repeating the interrogation for all elements of the flow field one thus achieves the quantitative velocity measurement and flow visualization. One of the earlier methods for quantitative flow visualization is known as the particle image velocimetry (PIV) method.[6,9] Double or multi-exposure images with a known time interval are taken on a single frame of film by a camera. The images are then optomechanically processed using the principle of Young's fringe. Unlike the PIV method, the information of the particle images in the whole field obtained in the DVV method is time-sequentially transferred directly to the computer memory and processed digitally to obtain the velocity field without the need of developing pictures as it is done with the film.

It is shown that the DVV method may provide the full field measurement without disturbing the flow other than light scattering particles seeded in the flow. Images are taken from the scattered light on the particles. In the present study, 15 frames of time-sequential images are taken through a charge-coupled device (CCD) video camera. These images are analyzed by the DVV method to provide the velocity vector field for each view. The particle streak picture for each view is also obtained using the particle streak velocimetry (PSV) method[10,11] and then compared qualitatively with the measured field from the DVV method. In the experiment the cylinder wall and bottom for test cell are made of clear plexiglass to facilitate the access of the light. The rotating flow is measured in the laminar region for $Re = 3200$ with Re defined based on the rotating speed and the radius of the lid. The thickness of the light sheet is adjusted to 10 mm for the side view so that flow motion on the illuminated plane can be captured. The reason a rather thicker light sheet is needed for the side view is that the swirl velocity is expected to be much stronger compared with the radial or axial velocity. From the velocity vector field measured by the DVV method, the overall flow structure, the pressure field, recirculation, stagnation and separation in the lid-driven rotating flow may be investigated quantitatively.

When the side view is taken by the CCD video camera, the image is radially ditorted because of the convex wall on a cylindrical test cell. Another important distortion is due to a curved image plane of the light sheet, which is generated by the thick lens effect of the cylindrical test section. Therefore, particle images recorded from the side view are strongly dependent on the rotating direction of

the lid and therefore seem like asymmetric even though the steady rotating flow itself is axisymmetric. The image must be corrected to produce the accurate data. Furthermore, near the wall much velocity information may be lost due to the so called total internal reflection of light at the interface between plexiglass and air. In order to avoid this phenomenon near the wall, the test cell is modified during investigation by placing a square-shaped side wall filled with water around the cylindrical test cell. Detail of the total internal reflection and the optical analysis about the modified test cell is described in APPENDIX.

2. Experimental System

In performing a quantitative flow visualization of the rotating flow, the major components of the experimental system are (1) test section, (2) light source and optics, (3) recording medium, (4) light scattering particle and (5) data processing system. The schematic image processing system is shown in Fig. 1.

From an optical source, a laser light is passed through an optical system such that a light sheet is illuminated in the test section. The test fluid, water, is seeded with small light scattering particles so that the particles move with the flow and scatter light from the laser sheet. The scattered light is detected by the recording device. In the present study the charge-coupled device (CCD) is chosen as the recording medium since the image recorded by CCD can be stored in a digitized form in computer. When the frame storage mode is set, the CCD is arranged in a 540 (H) ×480 (V) array with each pixel area measuring 23μm× 23μm and the time between frames is 1/30 s (30 Hz), which is selected for this study. The digitally recorded images are then analysed by the proposed digital vector velocimetry (DVV) method to determine the quantitative velocity for the whole field.

The basic geometry selected for the present study is a cylindrical cavity with the top lid driven to rotate at a steady angular rotation. Detailed drawing for the test cell for the lid-

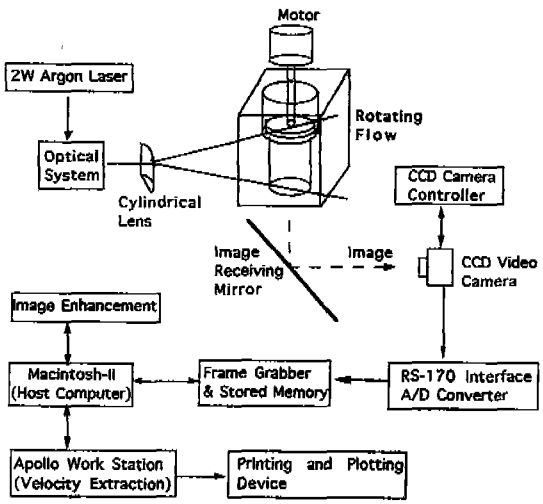

Fig. 1 Overall image processing system

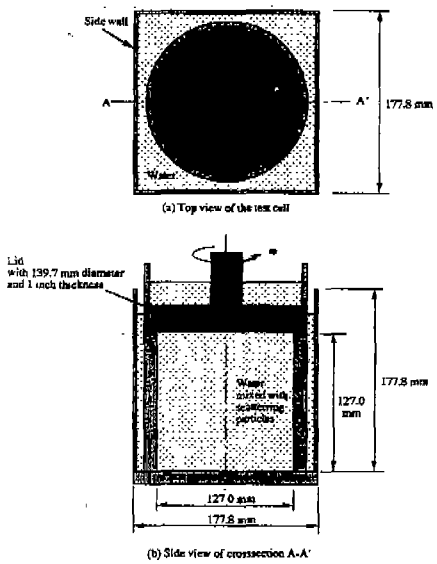

Fig. 2 Detailed drawing of test cell for lid-driven rotating cavity flow

driven rotating cavity flow is given in Fig. 2. To avoid the noise due to the reflection of light from the laser, all surfaces of the lid are coated with a black enamel paint.

The seeding particle chosen for the experiment in water is Pliolite VT, which is vinyl-toluene-butadiene copolymer. The mean diameter of the particles is 50 - 100 μm. The particles are insoluble in water and have an index of refraction of about n=1.6. With a specific gravity of 1.03, they may be considered neutrally buoyant.

Images obtained by the CCD video camera are fed into a microcomputer through a frame grabber interface board. During the process, the analog signals are converted into digital ones representing the flow field image. The data contained in the sequential flow images include displacement information of the particles and time interval between the flow images. During the experiment, noise in images may be generated by optical or electronical reasons from the system and by the particles that are moving in or out of the interrogation window. Before processing the digital data from the images, the noises must be reduced as much as possible. The data are in ASCII file format and ready to be used for quantitative velocity measurement by the digital vector velocimetry (DVV) method. Each image datum is a two-dimensional array of the dimension corresponding to the size of the interrogation window and every pixel has the integer value between 0 and 255 scaled by 8 bits or 256 gray levels.

3. Optical Distortion and Correction

The procedures for the correction of the optical distortion associated with the image created by the cylindrical plexiglass must be considered. The flow selected for investigation

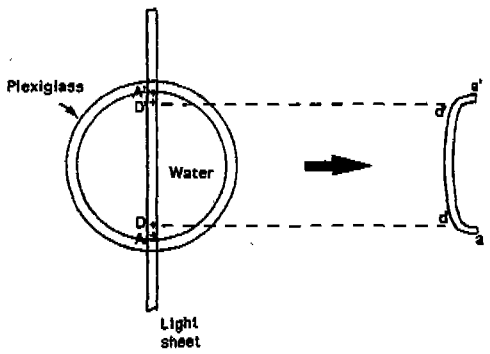

Fig. 3 Distorted image plane of side view

is a rotating flow in a cylindrical cavity driven by a lid. Therefore, one must correct any optical distortion in the images after the DVV method is implemented. An optical distortion in an image is created when one take a picture of the side view from the light sheet illustrated in Fig. 3, and the image plane is curved due to optical distortion in the radial direction.

Because water and plexiglass cylindrical wall behave as a thick non-Gaussian lens, analytical optical correction is difficult to be made. Instead a direct measurement of a physical reference scale, as shown in Fig. 4, in cylinder is conducted. The reference scale that has the markers coated with water-unsoluble black paint is positioned on the center inside the cylinder where the light sheet is located. The reference scale is immersed inside the test cell filled with water and the image of it from the side view is then recorded by the CCD video camera. Each location of the lines or markers on the scale is measured and is compared with the known undistorted scale. The position and displacement correction curves are then generated, as shown in Fig. 4. Once the correction curves are obtained, they are used as standards to recover the original radial position of the particle image and therefore the velocity magnitude from the dis-

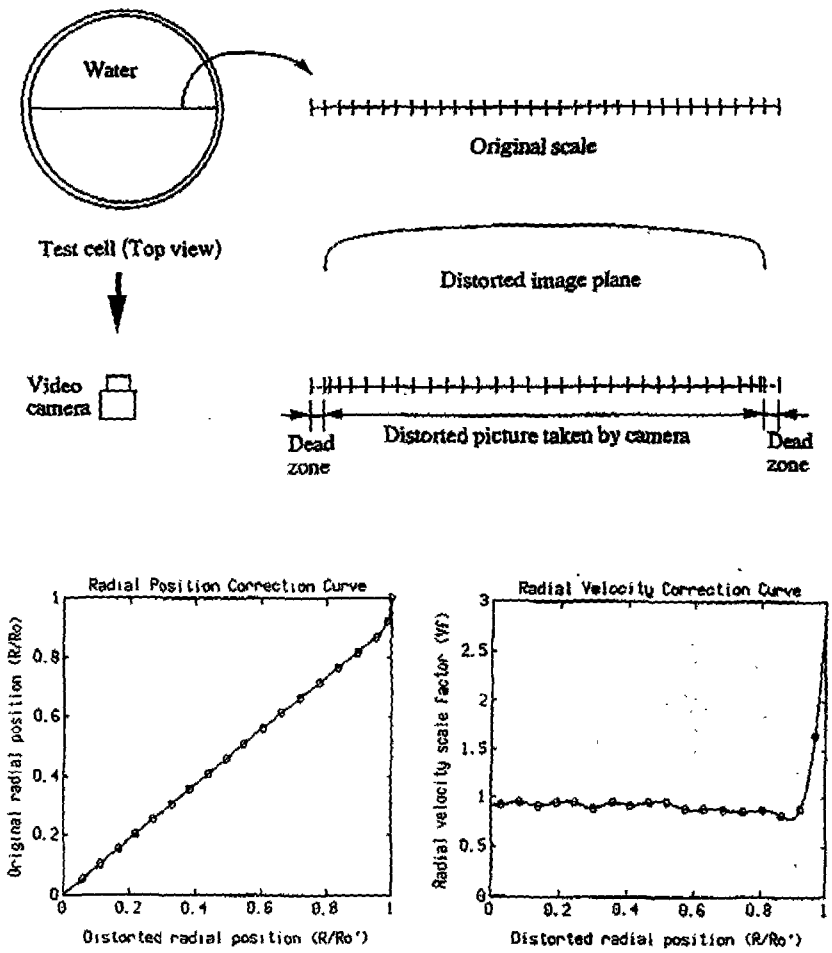

Fig. 4 Correction curves for lid-driven rotating cavity flow (Ro; original radius, Ro'; radius of distorted image)

torted image.

The particle location on the image is found to be only slightly distorted except that near the wall. When the light travels from the water to air through the plexiglass wall, the phenomenon of so-called total reflection may happen within some region near the wall (A-D and D'-A' region in Fig. 3) and therefore in this region no image can be obtained. This region is referred to as the dead zone in the present study. Detail of optical analysis on this phenomenon is given in APPENDIX.

Another correction is required in the measurement due to particle motion. In the steady rotating flow within an axisymmetric test cell, the side view image taken from crosssection A-A' is expected to be axisymmetric. However, the flow field recorded on the side view image is not symmetric. This is because the image records the particles moving into the light sheet on one side and moving out on the other side. This flow image is further distorted by the curved cylindrical geometry and the finite thickness of light sheet used. Let us consider typical side and top views of images for the axisymmetric flow rotating clockwise

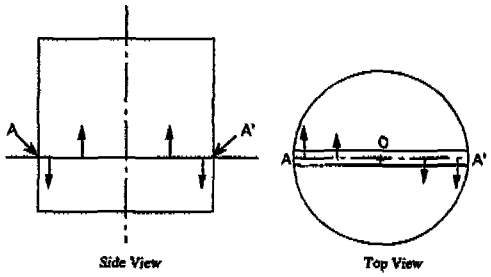

Fig. 5 Example of typical rotating flow

as in Fig. 5. Even though the figure is a little bit exaggerated, Fig. 6 shows that the image taken by a CCD camera is asymmetrical. Here an important problem of how the actual symmetric velocity field is recovered is raised. This problem can be solved using the average concept as follows.

Consider the flow rotating in the reverse direction, i.e., counterclockwise, with all other flow conditions remaining the same, as shown in Fig. 7. Then the velocity vectors of the picture taken from the image b-b' are also contaminated by the same amount of distortion as in clockwise rotation, but radially in the opposite direction. If we take average of the vectors on the images a-a' and b-b', the effect of the radial distortion is cancelled and the original, correct axial magnitudes of vectors are recovered. Therefore, the resultant

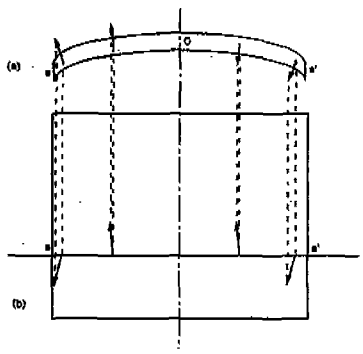

Fig. 6 Distorted image of velocity vectors
(a) Distorted image plane (Top view)
(b) Image taken by camera (Side view)

vector field is considered as axisymmetric, although it is still distorted in the radial position and displacement due to curved cylindrical geometry mentioned earlier.

After the actual velocity vectors at the original position are recovered using the correction curves that have been obtained in Fig. 4, they can be considered as an acceptable

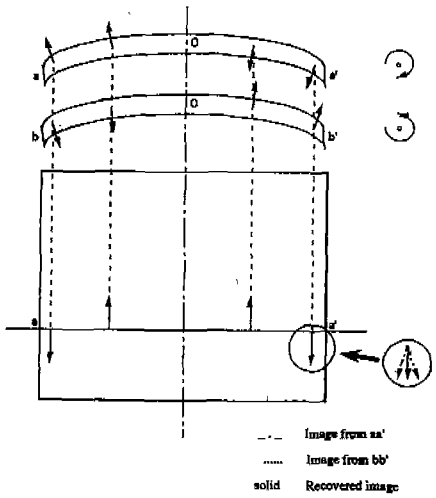

Fig. 7 Recovery of image using average concept

axisymmetric velocity vectors on the real light sheet A-A' of Fig. 3.

4. Analysis of Flow Visualization

In general, velocity information near the wall is very important in fluid mechanics. Thus we need to find a remedy to recover the lost velocity data in the so called dead zone near the cylindrical wall. For this purpose, the square-shaped plexiglass side walls are placed outside the original plexiglass cylindrical test cell. Water is filled in the space between the cylinder wall and the side wall. Because the configuration of the test cell is modified, other correction curves for radial

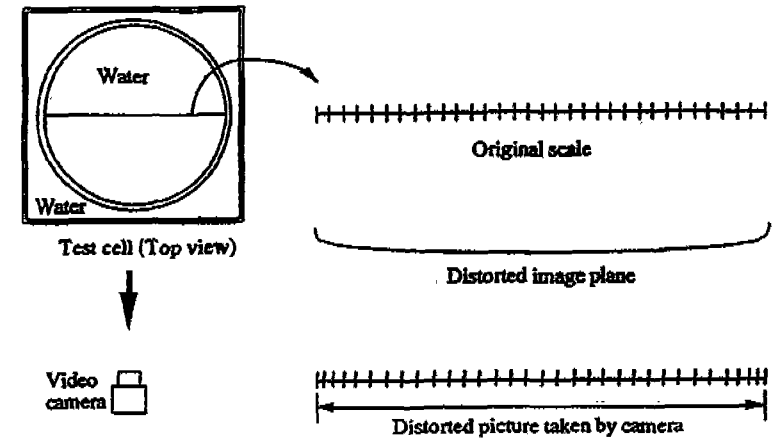

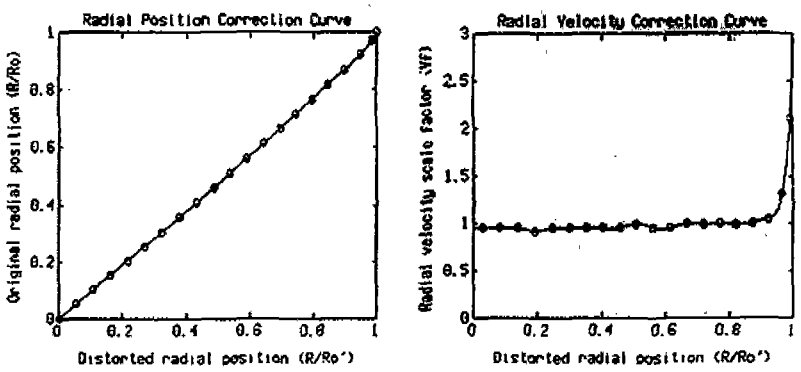

Fig. 8 Correction curves for lid-driven rotating flow with side wall (Ro; original radius, Ro'; radius of distorted image)

position and velocity need to be prepared. The schematic diagrams of the top view of the test cell and the corresponding correction curves are shown in Fig. 8.

The detail of the optical background for the modified test cell is described in APPENDIX. From this analysis it can be shown that the dead zone near the wall is eliminated and the whole velocity field may be captured. Therefore in this study the test cells with side wall are used for quantitative measurement of velocity field by the DVV method and the detailed description of experimental measurements is given in the following.

The dimension of the flow domain, 127 mm diameter by 127 mm depth, taken by the CCD video camera is 421×211 pixels in this configuration of the test cell. The size of the interrogating window is 31×31 pixels or 9×9 mm^2 except near the boundary including the axis, where the dimension of the window is set as 31×21 or 21×21 pixels to increase the resolution near the boundary with 21 pixel length (≈6 mm) in the normal direction to the boundary. The Reynolds number (or angular speed) of $Re = 3200$ (10 rpm) is selected for quantita-

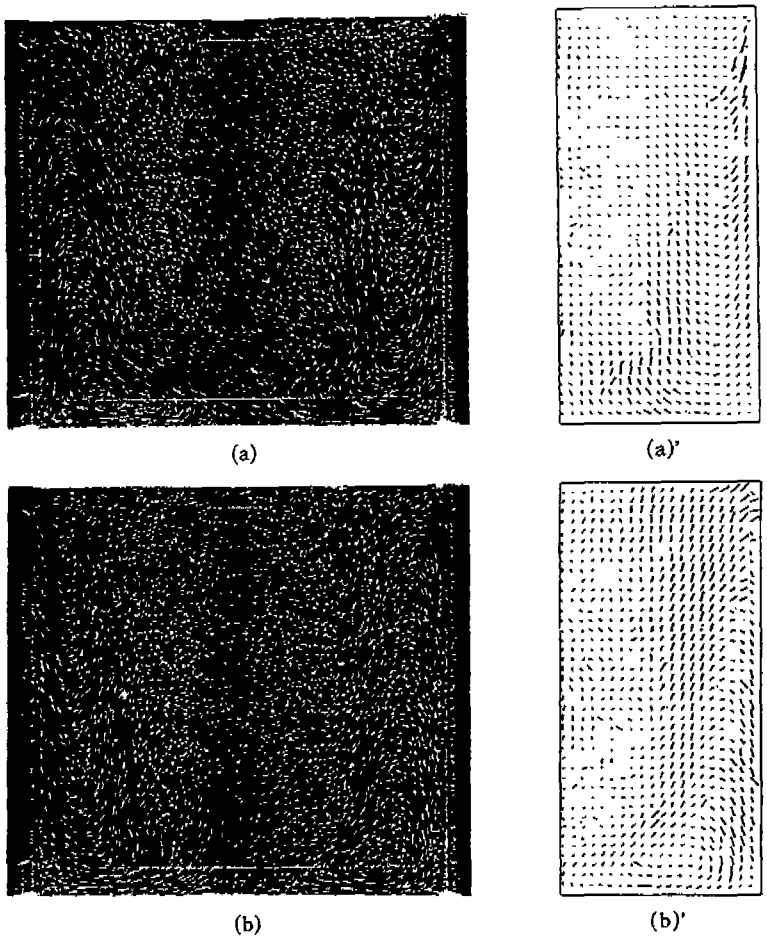

Fig. 9 Particle streak view and result of DVV measurement of lid-driven rotating flow with side wall (ω=10 rpm).
(a) & (a)' Counterclockwise rotation of lid
(b) & (b)' Clockwise rotation of lid

tive investigation of the lid-driven rotating flow.

The velocity vector plots from the digital vector velocimetry (DVV) method for angular speed of 10 rpm are compared with the qualitative pictures obtained using the particle streak velocimetry (PSV) method in Fig. 9, which is obtained by the CCD camera with an exposure time of 0.8 s to create the particle streak image. It is seen that the two flow patterns with the opposite directions of lid rotation are not symmetrical and look totally different from each other. The actual flow pattern should be symmetric according to axisymmetry of the domain. For each case, the velocity vector pattern measured from the DVV method reveals good agreement with the particle streak view. Thus both of the PSV and the DVV measurements seem to be in agreement and convincing. Fig. 10 shows the corrected side view through the optical corrections. Velocity vector plot (a) is a recovered

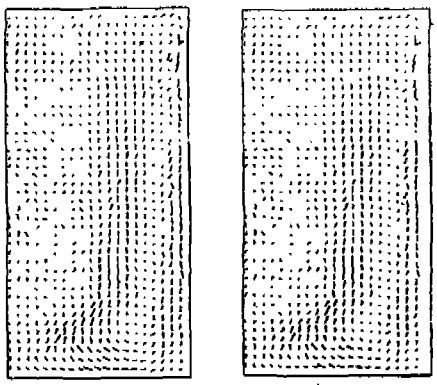

Fig. 10 Corrected side view flow field of lid driven rotating flow with side wall (ω=10 rpm). (a) Recovery of axisymmetric flow using average concept. (b) Final distortion-corrected axisymmetric flow field.

axisymmetric flow field by taking average of images (a)′ and (b)′ in Fig. 9. The final axisymmetric flow field after taking correction of the rotational direction and correcting the radial distortion using the correction curves given in Fig. 8 is shown in plot (b) of Fig. 10.

As expected, many velocity data near the wall are recovered using the modified test cell while without the side wall they are lost in the dead zone. The experimental data obtained are compared with the numerical results by the FAM in Fig. 11. Numerical calculation for the lid-driven rotating cavity flow is conducted with staggered system of 42×22 grids, and results of velocity vector, stream function and pressure distribution are given in the figure. The comparison reveals good agreement with each other.

5. Conclusion

The optical analysis is considered to improve the accuracy of the DVV method in case of test cell including convex cylindrical wall and to apply to the lid-driven rotating flow.

With the cylindrical geometry of the test cell, many velocity data in the region near the wall, typically about 10 % of the total velocity data, are lost due to the total internal reflection occurring in the interface between the plexiglass and air. The region in which the image can not be seen from the side view is called as the dead zone in the present study. In order to eliminate the dead zone, the test cell is modified by placing a square-shaped container filled with water around it. With the modified test cell, the whole field image including near wall images may be captured by the DVV method.

As a post-treatment of velocity field of the side view obtained from the DVV method, optical distortion due to the presence of the convex geometry of the plexiglass wall is corrected. The correction includes two steps. The first step is to recover the axisymmetric flow by taking average of the two velocity fields with opposite directions of rotation of the lid. The second step is to achieve the radial distortion-free axisymmetric flow field using the correction curves prepared for the rotating flows. After corrections, the final accurate axisymmetric velocity field for the side view is obtained. The quantitative measurement of the DVV system with the correction of optical distortion shows good agreements with numerical simulations.

Reference

1. Hesselink, L., "Digital Image Processing in Flow Visualization," Annual Review of Fluid Mechanics, Vol. 20, pp. 421-485, 1988.
2. Adrian, R. J., "Particle-Imaging Techniques for Experimental Fluid Mechanics," Annual Review of Fluid Mechanics, Vol. 23, pp. 261-304, 1991.

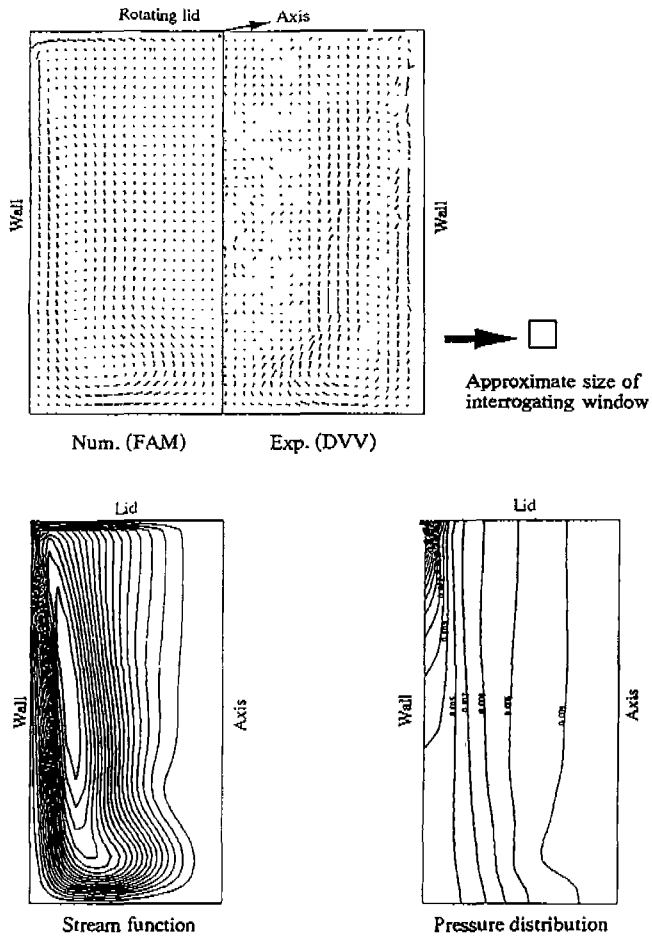

Fig. 11 Comparison of numerical results and experimental data of side view for lid-driven rotating cavity flow (Re=3200 or ω=10 rpm)

3. Kim, Y. G., "Development of Digital Vector Velocimetry Method and Its Application to Rotating Flows," Ph. D. Dissertation, Mechanical Engineering., The University of Iowa, 1991.
4. Kim, Y. G. and Chen, C. J., "Quantitative Flow Measurement and Numerical Simulation of Lid-Driven Rotating Cavity Flow," 1992 ASME Winter Annual Meeting, November, Anaheim, CA, 1992.
5. Chen, C. J., Kim, Y. G. and Walter, J. A., "Progress in Quantitative Flow Visualization and Imaging Process," Atlas of Visualization, Vol. 1, 1993.
6. Chen, C. J. and Chen, H. C., "The Finite Analytic Method:Vol. IV," IIHR Report, No. 232, Iowa Institute of Hydraulic Research, Iowa City, 1982.
7. Chen, C. J. and Chen, H. C., "Finite Analytic Numerical Method for Unsteady Two Dimensional Navier-Stokes Equation," Journal of Computational Physics, Vol. 53, No. 2, pp. 209-226, 1984.
8. Adrian, R. J., "Electrooptical Image Shifting for Particle Image Velocimetry," Applied Optics, Vol. 27, No. 20, pp. 4216-

4220, 1988.
9. Landreth, C. C., Adrian, R. J. and Yao, C.-S., "Double Pulsed Particle Image Velocimetry with Directional Resolution for Complex Flows," Experiments in Fluids, Vol. 6, pp. 119-128, 1988.
10. Dimotakis, P. E., Debussy, F. D. and Koochesfahani, M. M., "Particle Streak Velocity Field Measurements in a Two-Dimensional Mixing Layer," Physics of Fluids, Vol. 24, No. 6, pp. 995-999, 1981.
11. Walter, J. A. and Chen, C. J., "Flow Visualization of Particle Streaks in Offset Channel Flow by a Direct CCD Imaging Process," The Winter Annual Meeting of ASME, San Francisco, CA, FED-Vol. 85, pp. 115-120, 1989.
12. Pedrotti, F. L. and Pedrotti, L. S., Introduction to Optics, Prentice-Hall, Englewood Cliffs, NJ, 1987.

APPENDIX: Optical Analysis for Image from Cylindrical Test Section

It is observed that with the cylindrical test cell many velocity data near the wall are found to be lost. In the study this region is called as the dead zone. The image from a particle inside the dead zone can not be captured because the total internal reflection happens at the interface where the scattered light travels from plexiglass to air.

In general, velocity information near the wall is very important in fluid mechanics. Thus we need to find a remedy to recover the lost velocity data near the cylindrical wall. For this purpose, the square-shaped plexiglass side wall is placed outside the original plexiglass cylindrical test cell. Water is filled in the space between the cylinder wall and the side wall.

A. Analysis of Optical Path for Test Cell without Side Wall

The optical path from the scattered light from the illuminated particle to the CCD image is analyzed. The test cell considered is as shown in Fig. A-1 which is a cylindrical plexiglass, with optical index of refraction n_p, containing water with refraction index n_w. Outside the cylinder is air with refraction index n_a. This is the case for the test cell without side wall. In order to understand the optical path through the test cell the following analysis is performed.

When the ray travels from plexiglass ($n_p = 1.6$) to air ($n_a = 1.0$), the critical angle can be solved as

$$\theta_c = \sin^{-1}\left(\frac{1.0}{1.6}\right) = 38.7^\circ \qquad (A-1)$$

The paths of the light rays are categorized into three cases. One is the path of the ray A from the particle near the axis, and another ray C is from the particle near the cylinder wall, and the other ray B is from the intermediate region.

Snell's law requires that ray A in Fig. A-1,

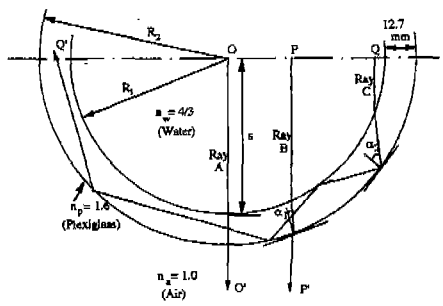

Fig. A-1 Refraction of rays at test cell

incident normal to the surface from point O, is transmitted without change of direction regardlessly of the ratio of refractive indices. For particles near point O, Gaussian lens formula[12] for interface between substances holds.

$$\text{Water} \rightarrow \text{Plexiglass}: \frac{n_w}{s} + \frac{n_p}{s'} = \frac{n_p - n_w}{-R_1} \quad (A-2)$$

$$\text{Plexiglass} \rightarrow \text{Air}: \frac{n_p}{(-s' + 0.5\,\text{inch})} + \frac{n_a}{s''} = \frac{n_a - n_p}{-R_2} \quad (A-3)$$

where s is the object distance, s' is the intermediate image distance due to the interface between water and plexiglass, s" is the final image distance from the interface between plexiglass and air, and R_1 and R_2 are the radii of curvature at each interface. If the sign of the image distance is positive, the image is located at the distance from the interface in the direction of the original light. In the present study, R_1 = 2.5 inches, R_2 = 3.0 inches and s = 2.5 inches.

Equations (A-2) and (A-3) give us s" = -3.0 inches, which means that the images of the objects near point O are focused at original locations. If s" is set to be an infinite value, then the length s = 12.496 inches is obtained, which is referred to as the front focal length. Consider now the optical path of ray B from point P located apart from the center point O.

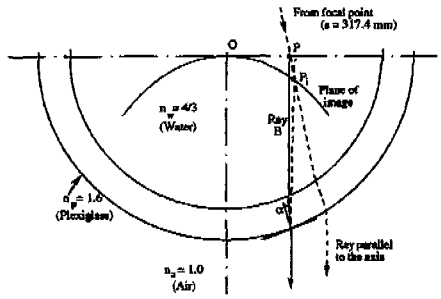

Fig. A-2 Creation of image of offaxis object P

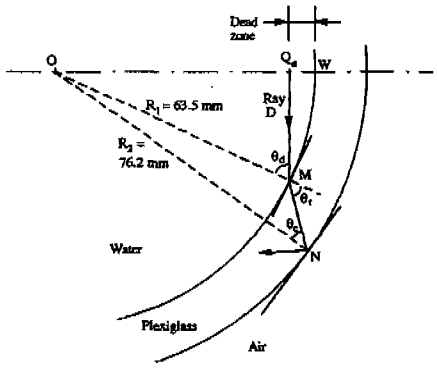

Fig. A-3 Illustration of the dead zone

The image of point P is seen as P_i which is obtained in a manner shown in Fig. A-2.

Also the case of ray C is shown in Fig. A-1. Ray C from point Q refracts at the first interface between water and plexiglass, and may experience the total internal reflection at the second interface between plexiglass and air if the angle of incidence, α_2, is greater than critical angle of incidence (38.7°), as shown in Fig. A-1. Therefore the image of Q can not be obtained by taking the picture. The region where the images of the objects created by rays similar to ray C are lost in this manner is called the dead zone.

The region of the dead zone can be determined analytically from an optical analysis. Assuming that the ray D from point Q_d is the closest ray to the wall, W, that can be imaged from the side view by the CCD camera, the ray D from that point travels along the path drawn in Fig. A-3. Applying the trigonometric rule to ΔOMN, we have the relation:

$$\frac{R_1}{\sin\theta_c} = \frac{R_2}{\sin(180^\circ - \theta_r)} \quad (A-4)$$

From the Snell's law at point M,

$$n_w \sin\theta_d = n_p \sin\theta_r \quad (A-5)$$

Equations (A-4) and (A-5) give us θ_d =

64.2°, which means that the limiting point Q_d is located at $R = R_1 \sin\theta_d \approx 0.90\ R_1$. Therefore, it is concluded that the dead zone for the side view of the given test cell is in the region of $0.9R_1 < R < R_1$ and no image can be obtained in the range, which shows that the image near the cylinder wall, about 10 % of the total image, is lost due to the dead zone just analyzed.

B. Analysis of Optical Path for Test Cell with Side Wall

To modify the test cell so that we may capture the image near the wall, a side wall that is a flat wall container is added around the cylinder, as shown in Fig. B-1. The purpose of using the side wall is to eliminate the dead zone defined in the previous section. The side wall, with 0.25 inch thickness of plexiglass plates, is placed around the cylindrical wall to form a square-shaped side wall and the space between the two walls is filled with water to change the optical path from the near wall region.

As explained in the section A, the critical interface for the dead zone is the one from plexiglass to air in Fig. A-1. If air is replaced by water, the critical angle of incidence (θ_{cs}) becomes much larger than that without the side wall. The critical angle for the test cell with side wall is

$$\theta_{cs} = \sin^{-1}\left(\frac{4/3}{1.6}\right) = 56.4^\circ \qquad \text{(B-1)}$$

In order to verify whether the dead zone is eliminated or not, the most extreme case, i.e., at point W just near $R = R_1$, is investigated, as shown in Fig. B-1.

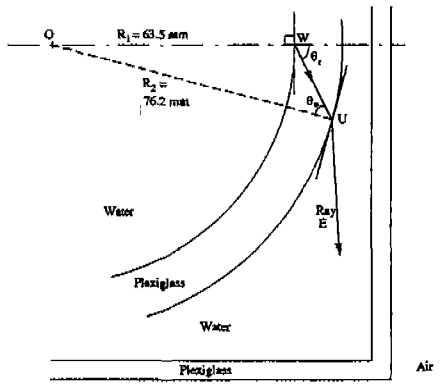

Fig. B-1 No dead zone with the side wall

The light ray E from point W which travels along the path through the cylinder and water is depicted in the figure. ΔOUW gives us the following relation by the trigonometric rule:

$$\frac{R_1}{\sin\theta_o} = \frac{R_2}{\sin(180^\circ - \theta_r)} \qquad \text{(B-2)}$$

Also from Snell's law at point W, we have

$$\theta_r = \theta_{cs} = 56.4^\circ \qquad \text{(B-3)}$$

From Equations (B-2) and (B-3), we have θ_o = 44.0°, which is greater than θ_c but less than θ_{cs}. In other words, the ray from point W of the test cell with the side wall is refracted along the path of ray E and can be imaged by the CCD camera while the ray from W without the side wall is totally reflected at the interface between plexiglass and air. Therefore, we conclude that if the side wall is placed around the cylinder wall with water filled between the two walls, the whole velocity field may be captured without losing velocity information near the wall inside the cylinder.